2013년 8월

석사학위 논문

The dynamic interaction of Foxo3a with the 53BP1 regulates mammalian autophagy

조선대학교 대학원

생물신소재학과

공 옥 화

The dynamic interaction of Foxo3a with the 53BP1 regulates mammalian autophagy

2013년 8월 23일

조선대학교 대학원

생물신소재학과

공 옥 화

The dynamic interaction of Foxo3a with the 53BP1 regulates mammalian autophagy

지도교수 유 호 진

이 논문을 석사학위신청 논문으로 제출함

2013 년 4 월

조선대학교 대학원

생물신소재학과

공 옥 화

공 옥 화의 석사학위논문을 인준함

위원장　조선 대학교　교수 장 인 엽 인

위　원　조선 대학교　교수 이 정 희 인

위　원　조선 대학교　교수 유 호 진 인

2013 년 5 월

조선대학교 대학원

CONTENTS

RESULTS

DISCUSSION

REFERENCES

CONTENTS OF FIGURES

ABSTRACT

The dynamic interaction of Foxo3a with the 53BP1 regulates mammalian autophagy

Yu Hua Kong

Advisor : Prof. Ho Jin You Ph.D.

Foxo3a is a member of the Forkhead box-o transcription factor family, which modulates the expression of genes involved in DNA damage repair, apoptosis, autophagy and other cellular processes. Foxo3a is acetylated within cells and that the acetylation of Foxo3a is increased in response to H_2O_2. Recently, acetylation of Foxo3a by CBP and/or p300 has been identified as a novel regulatory pathway, although the exact consequences of acetylation remain unclear. In this study, we show that 53BP1 bind to Foxo3a protein and then Foxo3a controls the transcription of autophagy and apoptosis-related genes. We used 53BP1-siRNA in mammalian cells to demonstrate that repressed various Foxo3a modulates target-genes in celluar processes. We found that consequently decreased Puma and LC3 through repression of Foxo3a acetylation in 53BP1-siRNA U2OS cells. The 53BP1 silencing cells reduced autophagy, elevated reactive oxygen species (ROS) and mitochondria mass. The knockdown of 53BP1 expression increased the cell viability of U2OS cells in response to H_2O_2 treatment. Our data suggest that 53BP1 regulate autophagy through effects of Foxo3a transcription factors function. In conclusion, our study reveals a novel role of 53BP1 in modulation of autophagy activity through regulation of Foxo3a transcription factors function.

INTRODUCTION

Autophagy (from the Greek, “auto” oneself, “phagy” to eat) has been implicated in many physiological and pathological processes [1], and also it is a well-conserved cellular degradative pathway [2]. During autophagy, autophagosomes engulf cytoplasmic components, including cytosolic proteins and organelles to recycle the components for reuse [3, 4]. Most importantly, drugs that potentially modulate autophagy are increasingly being used in clinical trials, and screens are being performed for new drugs that can modulate autophagy for therapeutic purposes [23]. Accordingly, there is a growing scientific need to accurately identify, quantify, and manipulate the process of autophagy [5]. Concomitantly, a cytosolic form of LC3 (LC3-I) is conjugated to phosphatidylethanolamine to form LC3-phosphatidylethanolamine conjugate (LC3-II), which is recruited to autophagosomal membranes. Autophagosomes fuse with lysosomes to form autolysosomes, and sequestered intra-autophagosomal components are degraded by lysosomal hydrolases. At the same time, LC3-II in autolysosomal lumen is degraded. Thus, lysosomal turnover of the autophagosomal marker LC3-II reflects autophagic activity, and detecting LC3 by immunoblotting or immunofluorescence has become a reliable method for monitoring autophagy and autophagy-related processes, including autophagic cell death [2]. p70S6 kinase plays a central role during nutritional regulation of translation. p70S6K is activated by growth factors such as insulin, and by mammalian target of rapamycin (mTOR), which is it self regulated by amino acids [6].

53BP1 was identified through its ability to bind to the tumor suppressor protein p53 through 53BP1’s COOH-terminal 312 amino acids BRCT (Brca1 carboxyl-terminus) repeats [16, 17], which are found in many DNA damage response proteins. 53BP1 is a key DNA repair factor that plays a pivotal role in defining DNA double-strand breaks (DSB) repair pathway choice in G1 and S/G2 cell-cycle phases [22].

Reactive oxygen species (ROS) are generally small, short-lived and highly reactive

molecules, formed by incomplete one-electron reduction of oxygen. ROS include oxygen anions, free radicals, such as superoxide and hydroxyl radical, and peroxides, such as hydrogen peroxide (H_2O_2). Oxidative stress results from exposure to high levels of ROS, which are not detoxified by cellular antioxidizing agents, but low levels of ROS induce autophagy [8, 9]. ROS are normally detoxified by glutathione, thioredoxin, superoxide dismutase (SOD), and also by catalase and peroxidases, in the cytosol disruption [10, 11, 12]. Glutathione, the main redox buffer of the cell, is localized primarily in the cytosol, whereas SOD present both in the cytosol and in mitochondria, converts superoxide into H_2O_2, which is further detoxified into H_2O and O_2 by catalase or peroxidases, such as the glutathione peroxidase. Given the role of ROS in inducing autophagy, antioxidants serve as natural downregulators of this process [12]. The delicate balance between ROS production and elimination might lead to accumulation of ROS in the mitochondria, therefore mitochondria acts as the source for redox regulation of autophagy. Several studies implicate mitochondrial ROS in the induction of autophagy [9]. Mitochondria contain their own genome, which is a circular double-stranded DNA molecule of ~16 kb (mtDNA). Mammalian mtDNA contains 37 genes, which code for 13 polypeptide components of the respiratory chain as well as rRNAs and tRNAs necessary for intramitochondrial protein synthesis [18]. Mitochondria are the major source of ROS, together with the fact that mitochondria do not have the enzymes necessary for NER and protective histone wrapping. It has long been suspected that mtDNA is the prime and vulnerable target of ROS attack [19]. It is also suspected that mtDNA damage, if not repaired, leads to disruption of the electron transport chain and production of more ROS, which, in turn, leads to further mtDNA damage, hence the concept of a ‘vicious cycle’ of ROS production and mtDNA damage. The importance of mtDNA damage in ageing and age-associated diseases which have been supported by the observations that mtDNA damage increases with age and mitochondrial dysfunction is a common aetiology of many age-associated neurodegenerative diseases [20, 21]. Mitophagy is relevant to the mitochondrial theory of aging [13]. Mitochondria are a continuing source of ROS formation. These free radicals cause mtDNA mutations that

progressively accumulate, especially since DNA repair processes in mitochondria are less robust than in the nucleus. mtDNA mutations impair synthesis of key proteins for oxidative phosphorylation, leading eventually to bioenergetic failure and ultimately cell death [14]. Upon withdrawal of the proliferative stimulus, autophagy removes the excess peroxisomes. Such peroxisomal autophagy or pexophagy is clearly selective since autophagic degradation of other organelles does not accelerate [15]. Dysfunction of autophagy has been proposed as an underlying mechanism for neurodegenerative diseases, muscle diseases, cancer, and hepatic inflammation. Clearly, we have learned and will continue to learn a great deal from autophagy mechanism of organisms. The critical question is whether these lessons translate into predicted insights regarding the roles of autophagy in human disease [24]. For example, recent reports show that this form of autophagic cell death is activated in the nervous system in response to oxidative stress. In Parkinson's disease, oxidation of dopamine induces oxidative stress, autophagy and cell death [47].

Foxo3a is a member of the Forkhead box-O (FOXO) transcription factors. Activation of FOXOs can directly promote the transcription of genes involved in the extrinsic and/or intrinsic apoptotic pathways and autophagic pathways [7]. FOXO3a up-regulates Puma expression in response to cytokine or growth factor deprivation [44].

In this study, we focus on the connections between 53BP1 and Foxo3a, describing their central role as modulators of fundamental processes such as stress resistance, cell metabolism, autophagy and cell death, and highlighting the autophagic potential of the 53BP1-Foxo3a axis. Our data suggest that 53BP1 regulate autophagy through effects of Foxo3a transcription factors function. In conclusion, our study reveals a novel role of 53BP1 in regulation autophagic effector LC3-II activity through repression of Foxo3a transcription factors function.

MATERIALS AND METHODS

1. Maintenance of cell lines

U2OS (osteosarcoma) and HEK 293T cell lines were cultured as monolayers in Dulbecco's modified Eagle's medium (DMEM, Gibco-BRL, Grand Island, NY, USA). Cells were supplemented with 10 % fetal bovine serum (FBS, Cambrex Corp., East Rutherford, NJ, USA), penicillin and streptomycin (100 units/ml and 100 mg/ml, respectively, Invitrogen, Carlsbad, CA, USA). All cells were maintained in a humidified incubator containing 5 % CO_2 at 37 °C.

2. 53BP1-siRNA design and transfection

siRNAs transfection and knockdown of 53BP1 expression. The mRNA sequence was extracted from the NCBI Entrez nucleotide database. These target sites were investigated using a BLAST search (National Center for Biotechnology Information) to confirm that the sites were specific to the 53BP1. The sequences of the 18-nucleotide sense and antisense RNA are as follows: 53BP1 siRNA, 5'-GGACAAGUCUCUCAGCUAdTdT-3' (sense) and 5'-UAGCUGAGAGACUUGUCCdTdT-3' (antisense); Foxo3a siRNA, 5'-TGAAGGCACGGGC AAGAGCdTdT-3' (sense) and 5'-GCUCUUGCCCGUGCCUUCAdTdT-3' (antisense); Cells seeded in 100-mm plates were incubated and treated with siRNA to a final concentration of 400 pmol. The siRNA duplexes were transiently transfected into the cells using RNAiMAX (Invitrogen).

3. Western blot analysis

Cells were washed with ice-cold PBS and then lysed in NP-40 buffer (50 mM Tris-HCl, pH 7.4, 150 mM NaCl, 1 % NP-40, 1 mM PMSF, and protease inhibitors), extracts were mixed for 5 min and centrifuged at 13,000 rpm for 15 min at 4 °C. The supernatant was diluted with 5x

SDS sample buffer and boiled. After cellular protein concentrations were determined using the dye-binding microassay (Bio-Rad, Hercules, CA), and 20 ug of protein per lane were separated by SDS-polyacrylamide gel electrophoresis (SDS-PAGE). After SDS-PAGE, the proteins were transferred onto polyvinylidene difluoride membranes (PVDF). After electroblotting, the membranes were blocked 5 % skim milk in Tris buffer saline containing 0.05 % Tween-20 (AMRESCO) at room temperature for 2 hours. The membranes were rinsed with TBS-T and then incubated with appropriate primary antibodies in TBS-T at 4 ℃ overnight. All antibodies used in this study are 53BP1 mAb (H-300, 1:1,000 dilution), FKHRL1 (Foxo3a) mAb (H-144, 1:1,000 dilution), p21 mAb (H-164, 1:1,000 dilution), p53 mAb (DO-1, 1:1,000 dilution), GAPDH mAb (0411, 1:4,000 dilution), β-actin mAb (C4, 1:4,000 dilution) Cox-2 mAb (N-20, 1:1,000 dilution), Parkin (PRK8) mAb (1:500 dilution); were obtained from Santa Cruz Biotechnology. Antibodies against Puma mAb (#4976, 1:1,000 dulution), p-53BP1 mAb (ser1778, #2675, 1:1,000 dulution), mTOR mAb (#2972, 1:1,000 dilution), phospho-p70S6 Kinase mAb (Thr389, 108D2, 1:1,000 dilution), phospho-Foxo3a mAb (Ser318/321, 1:1,000 dilution), cleaved PARP mAb (Asp214, human specific, 1:1,000 dilution), cleaved caspase-7 mAb (Asp198, 1:1,000 dilution), cleaved caspase-3 mAb (Asp175, 1:1,000 dilution), cleaved caspase-8 mAb (Asp391, 1:1,000 dilution); were obtaines from cell Signaling Technology, Danvers, MA. Anti-LC3B (microtubule-associated protein 1 light chain 3B) clone 5F10 (nanotools). We followed manufacturer's protocol for dilution of all primary antibodies. The membranes were then washed, incubated with the biotinylated secondary antibodies (1:4,000 dilution) in a blocking buffer for 2 hours at room temperature, and washed again. The blotted proteins were developed using an enhanced chemiluminescence detection system.

4. Quantitative Real-Time (RT)-PCR

mRNA levels were quantified by Real-Time PCR using SYBR Green I Master kit (Takara Bio Inc.). PCR conditions consisted of a 10 sec 95 °C cycle followed by 5 sec at 95 °C and 40

cycles of 95 °C for 5sec, 60 °C for 35 sec and 95 °C for 15 sec, 60 °C for 1 min. Primers were as follows: 53BP1, 5'-AGGTGGGTGTTCTTTGGCTTCC-3' (forward); 5'-TTGGTGTTGAG GCTTGTGGTGATAC-3' (reverse); ATG8 (LC3), 5'-TCGGATCTCACTGTGGGCCAATTT -3' (forward); 5'-AACCATCCTCGTCCTTGTGCTCTT-3' (reverse); Foxo3a, 5'-GAACAGA CCAGCCACCTTCTCTT-3' (forward); 5'-TGAAGCAAGCAGGTCTTGGA-3' (reverse); GAPDH, 5'-TTCACCACCATGGAGAAGGC-3' (forward); 5'-GGCATGGACTGTGGTCAT GA-3' (reverse); catalase, 5'-GCAGATACCTGTGAACTGTC-3' (forward); 5'-GTAGAATG TCCGCACCTGAG-3' (reverse); MnSOD2, 5'-ACTGCAAGGAACAACAGGCC-3' (forward); 5'-TCCCACACATCAATCCCCA-3' (reverse); GPX 5'-CCTCAAGTACGTCCG ACCTG-3' (forward); 5'-CAATGTCGTTGCGGCACACC-3' (reverse); human mitochondrial DNA (3212-3319), 5'-CACCCAAGAACAGGGTTTGT-3' (forward); 5'-TGGCCATGGGTA TGTTGTTAA-3' (reverse); 18S rRNA (1546-1650), 5'-TAGAGGGACAAGTGGCGTTC-3' (forward); 5'-CGCTGAGCCAGTCAGTGT-3' (reverse).

5. Cytotoxicity Assay by MTT

The cell cytotoxicity was also assessed using a 3-4,5-dimethylthiazol-2,5-diphenyl tetrazolium bromide (MTT)-based colorimetric assay. The tetrazolium salt, MTT and the corresponding MTT formazan were both obtained from Sigma. Solvents used were phosphate-buffered saline (PBS) for 5 mg/ml. U2OS cells (1 x 10^4) were seeded in a 96-well plate. After 24 hour, cells were treated with H_2O_2 (0 to 160 uM) for 24 hours. 10 ul of 5 mg/ml MTT solution was added per well, and the plate reincubated at 37 °C in 5 % CO_2 for a further 4 hour. The purple formazan crystals were allowed. The medium containing MTT was removed, and dimethyl sulfoxide (DMSO) was added. Cells were incubated for 15 min room temperature with gentle shaking. Optical density measurements were carried out using Titertek Multiskan plate reader (ELISA reader) at 570 nm, with a fixed wavelength filter. The number of live cells

per well was calculated as a percentage of the control thus measuring cell survival after drug exposure. A dose-response curve was plotted for each drug.

6. Flow cytometry by PI staining

The U2OS cells were collected and washed with cold PBS once and suspension, then vortexed as 100 % Ethanol (-20 °C storage) was added to final 70 %. Fixed cells were stored at 4 °C for 30 minutes, and cells were washed with cold PBS to remove residual Ethanol, pelleted, and resuspended in PBS containing propidium iodide (Sigma; 50 mg/ml) and following digestion with RNase A essentially as described, addition of RNase A (Sigma) at a final concentration of 50 ug/ml, and incubated for 15 min at 37 °C. The stained cells were analyzed by flow cytometry. At least 10,000 events were analyzed, and the percentage of cells in sub-G_1 population was calculated. Aggregates of cell debris at the origin of histogram were excluded from the sub-G_1 cells. Forward light scatter characteristics were used to exclude the cell debris from the analysis. Apoptotic cells were determined by their hypochromic, subdiploid staining profiles.

7. LC3 immunofluorescence staining

Control-siRNA and 53BP1-siRNA U2OS cells cultured on cover slips coated with poly-L-lysine (Sigma). The cells were then washed twice with PBS, fixed with 4 % paraformaldehyde for 10 min and ice-cold 98 % Methanol for 5 min, at room temperature. Next, the cover slips were washed three times with PBS and then blocked with 1 % BSA and 5 % horse serum in PBS for 2 hours at room temperature. The cells were immunostained with primary antibodies directed against various proteins overnight at 4 °C. Next, the cells were washed with PBS and then stained with Alexa Fluor 488 nm (green, Molecular Probes) or Alexa Fluor 594 nm (red, Molecular Probes) conjugated secondary antibodies as appropriate. After washing, the cells were mounted using Vectashield mounting medium with 4,6-diamidino-2-phenylindole

(DAPI; Vector Laboratories, Burlingame, CA, USA). Fluorescence images were taken under a confocal microscope (Zeiss LSM 510 Meta; Carl Zeiss, Jena, Germany) using a x 60 1.4 NA oil immersion objective using the same instrument settengs for each image. Image analyzed with Zeiss LSM Image Examiner software (Carl Zeiss).

8. Mitochondrial staining

Cells cultured on cover slips pretreated with 5 mg/ml poly-L-lysine (Sigma), After 24 hour, cells were prepared for microscopy by incubation with 200 nM of a mitochondrion-specific dye MitoTracker® Red CMXRos, the dye stock solutions (1 mM, dissolved in DMSO) were stored at -20 °C. To stain active mitochondria. Dilute the 1 mM MitoTracker® Red CMXRos stock solution to the final working concentration in growth medium, cells were stained for 15 min at 37 °C. The cells were then washed three times in PBS, fixed with 4 % paraformaldehyde for 10 min and ice-cold 98 % Methanol for 5 min, the cover slips were washed three times with PBS. After washing, the cells were mounted using Vectashield mounting medium with 4,6-diamidino-2-phenylindole (DAPI; Vector Laboratories, Burlingame, CA, USA). Fluorescence images were taken using a confocal microscope (Zeiss LSM 510 Meta; Carl Zeiss, Jena, Germany), and analyzed with Zeiss LSM Image Examiner software (Carl Zeiss).

9. Measurement of mitochondrial ROS by FACS analysis

Mitochondria associated ROS levels were measured by staining cells with MitoTracker Red CM-H2XRos (Molecular Probes/Invitrogen). MitoTracker Red CM-H2XRos dilution by DMSO (1 mM stock concentration). Cells were cultured at 37 °C, 5 % CO_2 for 24 hours. After 24 hours, suction media and cells were washed with pre-warmed phosphate-buffered saline (PBS, pH 7.4) solution, and stained by MitoTracker Red CM-H2XRos dye 500 nM in full media, incubated in the dark for 30 min at 37 °C, 5 % CO_2. Cells were then washed with PBS

solution, trypsinized, and resuspended in PBS solution for FACS analysis. The fluorescence signal was recorded on the FL1 (green) channel and analyzed by using Cell Quest software.

10. Mitochondrial fraction

The Cultured cell were suspended in 250 ul cytosol buffer, and incubate on ice (cytosol buffer: 10 mM HEPES pH 7.9, 1.5 mM $MgCl_2$, 0.2 mM DTT, 0.4 % NP-40, protease inhibitor); lysed for 10 times cell passing through a 25 gauge needle fitted syringe (1cc). Centrifuge for 5 min at 8,600 rpm (eppendorf centrifuge 4 °C). Supernatant was centrifuge at utra 80,000 rpm for 15 min at 4 °C (Mitochondria), and add cytosol buffer to pellet (Nucleus) and resuspention, centrifuge at 8,600 rpm for 5 min pellet washing with lysis buffer, add NP-40 buffer (1 % NP-40, 50 mM, Tris-HCl pH 7.5, 150 mM, NaCl, protease inhibitor) and centrifuge at 13,000 rpm for 30 min supernatant is nucleus protein. Mitochondria pellet washing with and cytosol buffer. Centrifuge at 80,000 rpm for 15 min at 4 °C. Pellet lysed for NP-40 buffer and centrifuge at 13,000 rpm for 30 min. Supernatant contains mitochondrial proteins.

11. RNA isolation and cDNA synthesis

The Total RNA was extracted with TRI-zol (Invitrogen) and cDNA was synthesized from the extracted RNA using M-MLV reverse transcriptase (Invitrogen).

Add 1 ml of Trizol reagent to 60-mm dish, suspened in microtube and stand for 5 min, Add 0.2 ml (0.2 Vol) chloroform and shake vigorously by hand for 15 sec and incubate for 3 min at RT, centrifuge 12,000 rpm for 15 min at 4 °C transfer supernatant to a new microtube and add 0.5 vol (500 ul) isopropanol, mix and incubate for 10 min at RT, centrifuge 12,000 rpm for 10 min at 4 °C, Discard supernatant. (Very carefully, because can loss pellet). Add 70 % Ethanol 1 ml & Mix & Centrifuge 12,000 rpm for 5 min at RT, Discard supernatant (Very carefully,

perfectly) Remove supernatant and air dry for 5~10 min, Resuspend pellet with 50 ul DEPC (sotre at -70 °C). First-Strand cDNA synthesis using M-MLV RT. Add the following components to a nuclease-free microcentrifuge tube: 1 μl oligo (dT) (300 pmol), 4 μg total RNA of mRNA, 1 μl 10 mM dNTP Mix (10 mM each dATP, dGTP, dCTP and dTTP at neutral pH). Sterile, distilled water to 12 μl. Heat mixture to 65 °C for 5 min and quick chill on ice. Collect the contents of the tube by brief centrifugation and add: 4 μl 5x First-Strand Buffer, 2 μl 0.1 M DTT, 1 μl RNaseOUT™ Recombinant Ribonuclease Inhibitor (40 units/μl). Mix contents of the tube gently and incubate at 37 °C for 2 min. Add 1 μl (200 units) of M-MLV RT, and mix by pipetting gently up and down. Incubate 50 min at 37 °C. Inactivate the reaction by heating at 70 °C for 15 min.

12. Chromatin Immunoprecipitation Assay

Transcriptional factors analysis using the chromatin immunoprecipitation (ChIP) assay kit (Cell signaling). Cells are fixed with formaldehyde (Final concentration is 1 %). Mix and incubate for 10 min at RT. Add 10x glycine to each dish, incubate for 5 min at RT. For suspension cells, transfer cells to a conical tube, centrifuge at 1,500 rpm for 5 min at 4 °C, and wash pellet two times with 20 ml ice cold 1x PBS. Resuspend cells in 10 ml ice-cold Buffer A + DTT + PIC + PMSF. Incubate on ice for 10 min. Mix by inverting tube every 3 min. Pellet nuclei by centrifugation at 3,000 rpm for 5 min at 4 °C. resuspend pellet in 10 ml ice-cold Buffer B + DTT. Repeat centrifugation. Transfer sample to a microcentrifuge tube. Add 5 μl of Micrococcal Nuclease, mix by inverting tube several times and incubate for 20 min at 37 °C with frequent mixing to digest DNA to length of approximately 150-900 bp. Mix by inversion every 3 to 5 min. Stop digest by adding 100 μl of 0.5 M EDTA and placing tube on ice. Pellet nuclei by centrifugation at 13,000 rpm in a microcentrifuge for 1 min at 4 °C and remove supernatant. Resuspend nuclear pellet in 1 ml of 1x ChIP buffer + PIC + PMSF and split into two tubes of 500 μl. Incubate on ice for 10 min. Sonicate each tube of lysate with several

pulses to break nuclear membrane. Incubate samples for 30 sec on wet ice between pulses. Clarify lysates by centrifugation at 10,000 rpm in a microcentrifuge for 10 min at 4 ℃. Transfer supernatant to a new tube. This is the cross-linked chromatin preparation, cross-link histone and non-histone proteins to DNA. Antibodies specific to histone or non-histone proteins are added and the complex co-precipitates and is captured by Protein G agarose or Protein G magnetic beads. Cross-links are reversed, and DNA is purified and ready for analysis. Conditions: 95 ℃, 30 s; 95 ℃, 5 s, 60 ℃, 30 s. Ct value of each sample was normalized to the Ct value obtained from PCR reaction using the corresponding input genomic DNA as templates. Primer sequences were as follows: Human Puma FHRE: 5'-GCGCACAGGTGCCTCGGC-3'; 5'-TGGGTGTGGCCGCCCCT-3' [59].

13. Data Analysis

The data is represented as the mean ± SD. Statistical comparisons were carried out using an unpaired t test. p values < 0.05 were considered significant.

RESULTS

1. 53BP1 is related with H_2O_2-induced autophagy in U2OS cells.

LC3 is one of the major processes in autophagy pathway. LC3 exists in two molecular forms. LC3-I (18kD) is cytosolic, whereas LC3-II (16kD) binds to autophagosomes [25, 42]. The amount of LC3-II, which directly correlates with the number of autophagosomes increased after ROS level [25]. As a central element signaling cell growth and enhancing protein translation, the mTOR, when inhibited, induces autophagy [50]. Exposure of cells to H_2O_2 that induce genotoxic and oxidative stress causing repression of mTORC1 signaling. The cell repress mTORC1 to decrease protein synthesis and induce autophagy [49, 50]. We investigated the effect of 53BP1 knockdown on the formation of LC3-II. The western blot analysis using the specific antibody for LC3B, 53BP1, showed that 53BP1 inhibition by RNAi reduces LC3-II protein level in U2OS cells (Fig. 1A). LC3-II induced by H_2O_2, immunofluorescent staining showed that the mitochondria localization of LC3-II in response to 80 uM H_2O_2 was lower in 53BP1-siRNA transfected cells than in control-siRNA transfectants (Fig. 1B). Downstream targets of mTOR is the kinase p70S6 kinase (p70S6K) [51]. U2OS cells were transfected with control siRNA or 53BP1 siRNA, and then treated with 80uM H_2O_2 for the indicated time points. In control cells, phosphorylation of p70S6K reached a maximum at 30mins after H_2O_2 treatment and decreased. In constrast, 53BP1 knockdown U2OS cells exhibited a maximal level of phosphorylation of p70S6K until 8hr after H_2O_2 treatment. mTORC1 negatively regulates autophagy, and repression by ROS, autophagy increased in cells treated with H_2O_2 [49, 52]. The H_2O_2 treatment caused a modest increased in LC3-II in the control-siRNA transfected U2OS cells. In contrast, the LC3-II was not increase in response to H_2O_2 treatment 53BP1-siRNA transfected cells (Fig.1C). Our results suggest that 53BP1 has an important role in mTOR-mediated autophagy.

Figure 1.

A.

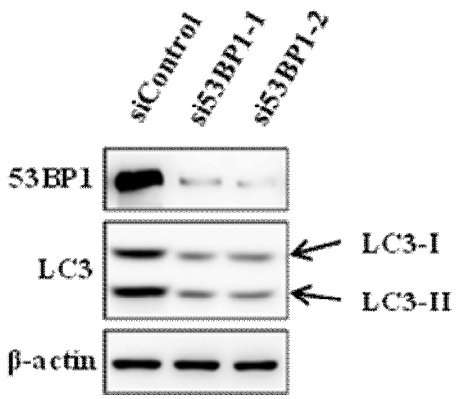
siControl
si53BP1-1
si53BP1-2
53BP1
LC3
LC3-I
LC3-II
β-actin

B.

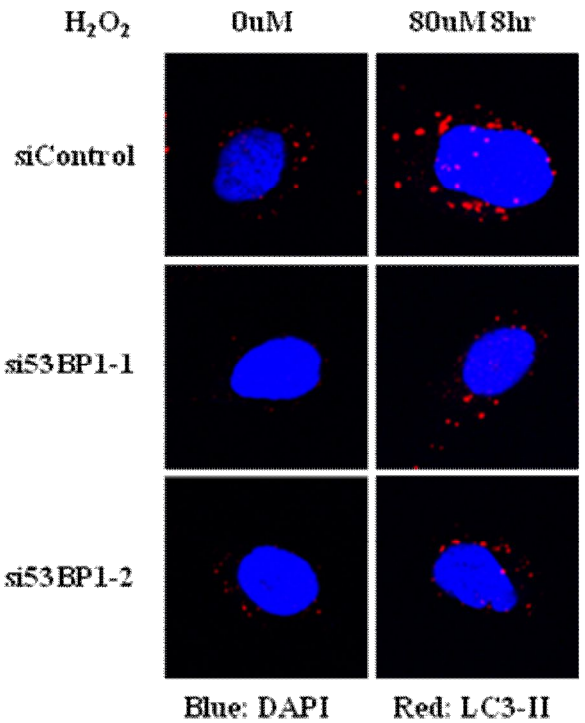
H2O2
0uM
80uM 8hr
siControl
si53BP1-1
si53BP1-2
Blue: DAPI
Red: LC3-II

C.

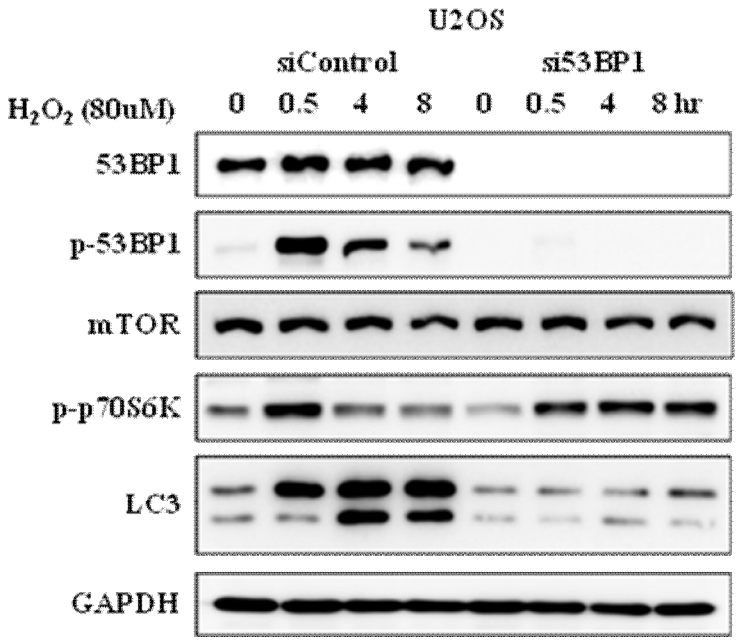

Figure 1. 53BP1 is related with H_2O_2-induced autophagy in U2OS cells.

(A) U2OS cells were stably transfected with the control-siRNA (siControl) and two different 53BP1-siRNA (si53BP1), analyzed by immunoblotting with an antibody for anti-53BP1, anti-LC3B (autophagy pathway genes), and β-actin (loading control). 53BP1 inhibition by RNAi reduces LC3 protein level. (B) LC3-II is found associated with autophagosome membranes in addition to the cytoplasm, U2OS cells transfected with control or 53BP1-siRNA, cells were treated with 80 uM H_2O_2 for 8 hour and fixed. Slide stained with anti-LC3B antibody, and analyzed by confocal microscopy. (C) transfection with control-siRNA or 53BP1-siRNA, the cells were treated with 80 uM H_2O_2 for the indicated times. Results are indicative of several different experiments with an antibody for anti-p-53BP1, anti-mTOR, anti-p-p70S6K, anti-LC3B, anti-GAPDH by Western blot analyses.

2. 53BP1 knockdown causes defects at H_2O_2-induced apoptosis.

We next studied the effect of 53BP1 on the H_2O_2-induced cytotoxicity of the U2OS cells by the MTT assay. The MTT values in the group treated with 0 to 160 uM H_2O_2 , stable control-siRNA and 53BP1-siRNA cells. The cell viability of 53BP1-siRNA cells was significantly higher than that of either control-siRNA cells (Fig. 2), indicating that the knockdown of 53BP1 expression increase the cell viability of U2OS cells in response to oxidative stress. We analyzed sub-G_1 DNA contents of control-siRNA and 53BP1-siRNA stable cells by flow cytometry after staining their nuclei with propidium iodide. The control-siRNA cells, which were treated with 0 to 160 μM H_2O_2, showed apoptotic sub-G_1 DNA contents from 3.91 % to 7.44 %. However, 53BP1-siRNA decreased the proportion of apoptotic sub-G_1 DNA content. The apoptotic sub-G_1 DNA contents of 53BP1-siRNA transfected cells ranged from 1.55 % to 3.33 % under similar same oxidative stress (Fig. 3A). Furthermore, the activation of caspases is one of the major processes in cell death [57]. In order to understand the effect of 53BP1 on H_2O_2-induced cell death in U2OS cells, the levels of cleaved caspase-3, cleaved caspase-7, cleaved caspase-8 and cleaved-PARP which are the key caspases in the cell death pathways [58], were examined by western blot analysis in control-siRNA and 53BP1-siRNA cells. The H_2O_2 treatment reduced the cleavage of procaspase-3, procaspase-7, cleaved caspase-8 and cleaved-PARP into the active subunit was clearly observed in the 53BP1-siRNA from 24 hour after H_2O_2 treatment. the level of cell viability higher in the 53BP1-siRNA transfected cell than in control-siRNA transfectants (Fig. 3B). Together, these results implicate that 53BP1 has a role in H_2O_2-induced apoptosis.

Figure 2.

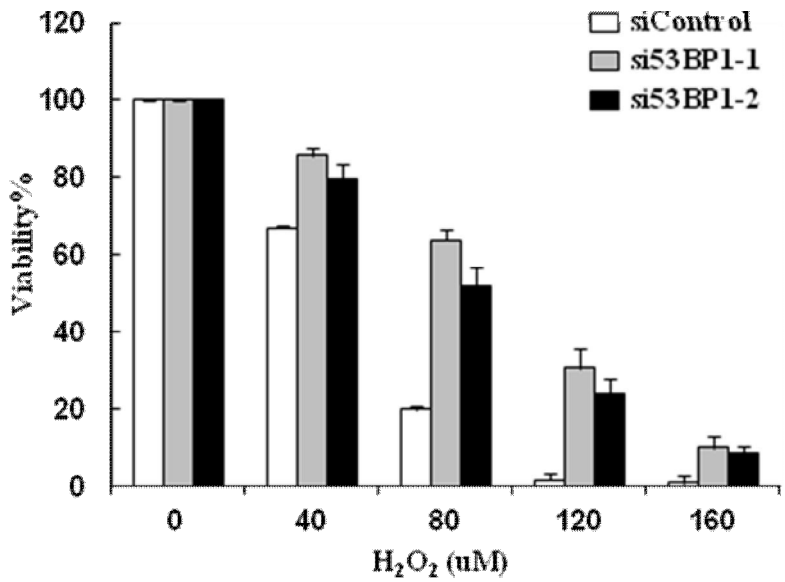

Figure 2. Effects of 53BP1 on cell viability.

The cytotoxic effect was demonstrated by cell counts using a MTT cell viability assay, control-siRNA and 53BP1-siRNA transfected cells were cultured to 70-80 % confluence, and treated with the 0 to 160 uM H_2O_2 for 24 hour, and the extent of cell death was assayed by MTT assay. Cell viability was determined as the percentage of total cell number that remained unstained. The values represent the means ± SD from three separate experiments.

Figure 3.

A.

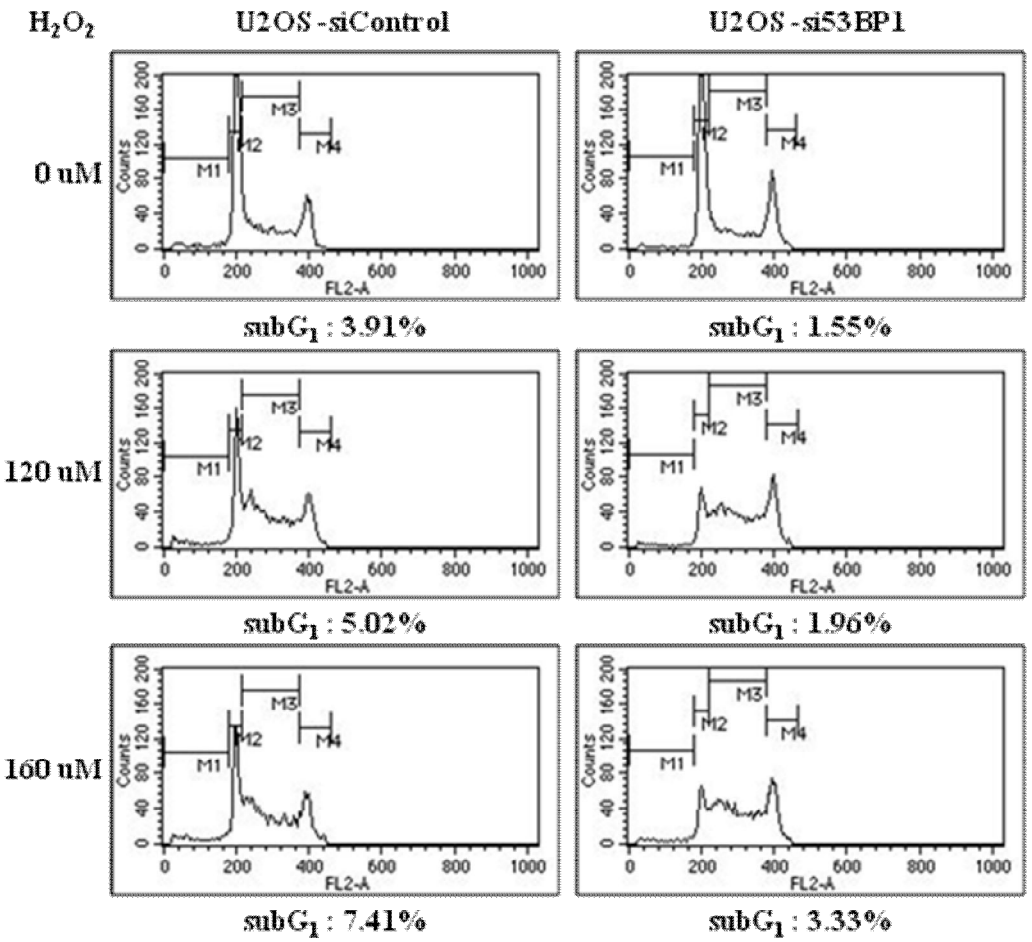
H2O2
U2OS - siControl
U2OS - si53BP1
0 uM
120 uM
160 uM
M1
M2
M3
M4
Counts
FL2-A
subG1 : 3.91%
subG1 : 1.55%
subG1 : 5.02%
subG1 : 1.96%
subG1 : 7.41%
subG1 : 3.33%

B.

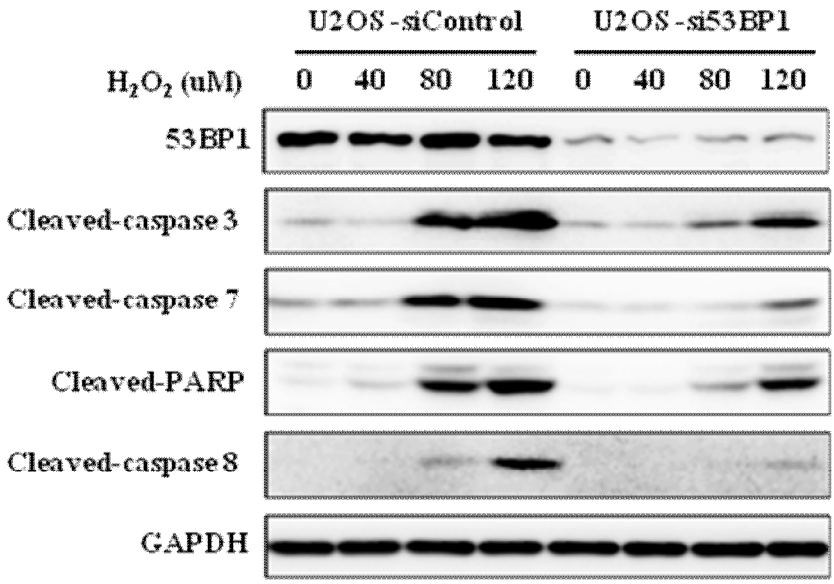

Figure 3. H_2O_2 induced cell death in 53BP1 knockdown cells.

(A) Apoptotic Sub-G_1 (M1) DNA contents were estimated by FACScan analysis FACS of H_2O_2-induced death in control-siRNA and 53BP1-siRNA U_2OS cells. Cells were showed that treatments with 0 to 160 uM H_2O_2 for 24 hour. Cells were fixed with Ethanol. The fixed cells stained by propidium iodide and following digestion with RNase A (Sigma). The stained cells were analyzed by flow cytometry. (B) The activated (cleaved) caspase-3, caspase-7, PARP and caspase-8 were detected by western blot analysis using specific antibodies (cleaved form) for caspase-3, caspase-7, cleaved-PARP, caspase-8. Cells were treated with 0, 40, 80, 120 uM H_2O_2 for 24 hour.

3. 53BP1 knockdown leads to induction of ROS and increased Mitochondrial mass.

Accumulation of ROS is an oxidative stress to which cells respond by activating various defense mechanisms. At low levels, ROS act as signaling molecules in various intracellular processes [9]. An important role for autophagy in the response to ROS is highlighted by the accumulation of oxidized proteins in cells. Mitochondria produce low levels of ROS as an inevitable consequence of oxidative metabolism and mitochondria have an essential role in autophagosome biogenesis [5]. We showed that the effect of 53BP1 for ROS and mitochondrial level in the 53BP1-siRNA U2OS cells. We quantified mitochondrial reactive oxygen species (mROS) levels using MitoTracker Red CM-H2XRos fluorescent probes, and increases in mROS measured by FACS analysis to directly evaluate the effect of 53BP1-siRNA cells on ROS production (Fig. 4A). As well as increases in mitochondrial mass as assessed by staining with MitoTracker Red CMXRos, that binds to mitochondria regardless of their membrane potential (Fig. 4B). Relative mtDNA level increased in 53BP1-siRNA treated U2OS cells, measured by real-time PCR (Fig. 4C). 53BP1-siRNA treated U2OS cells were stained with 200 nM MitoTracker® Red CMXRos and examined by confocal microscopy and increase mitochondrial mass and localization was analyzed (Fig. 4D).

Thus, loss of 53BP1 results in mitochondrial dysfunction and concomitant elevation of mROS levels and mitochondrial mass.

Figure 4.

A.

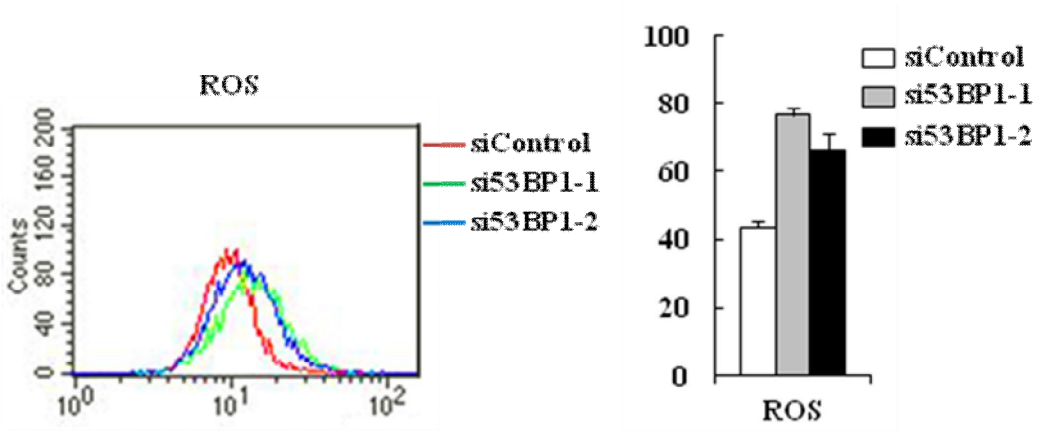
ROS
Counts
siControl
si53BP1-1
si53BP1-2
ROS

B.

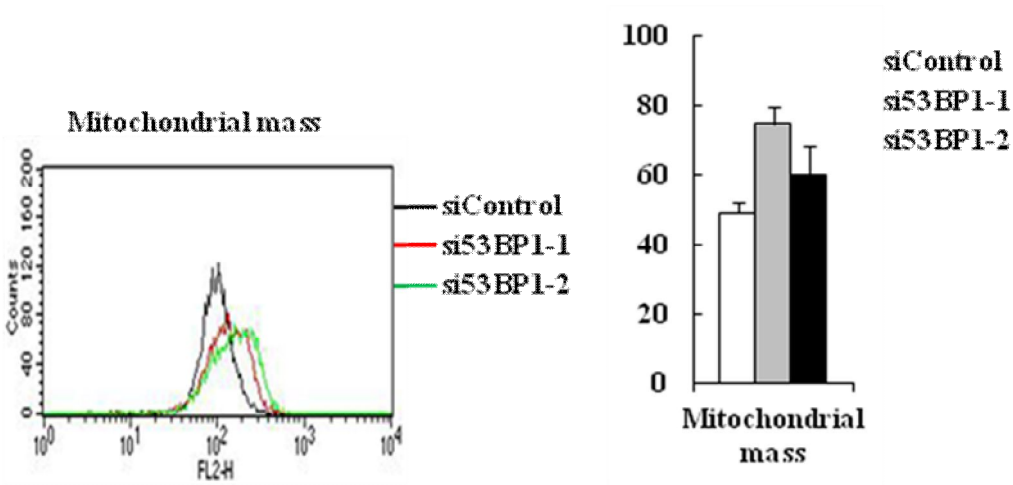
Mitochondrial mass
Counts
FL2-H
siControl
si53BP1-1
si53BP1-2
Mitochondrial mass

C.

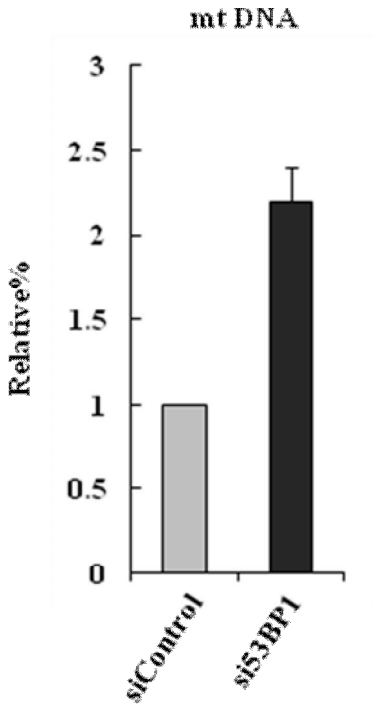
mt DNA
Relative%
3
2.5
2
1.5
1
0.5
0
siControl
si53BP1

D.

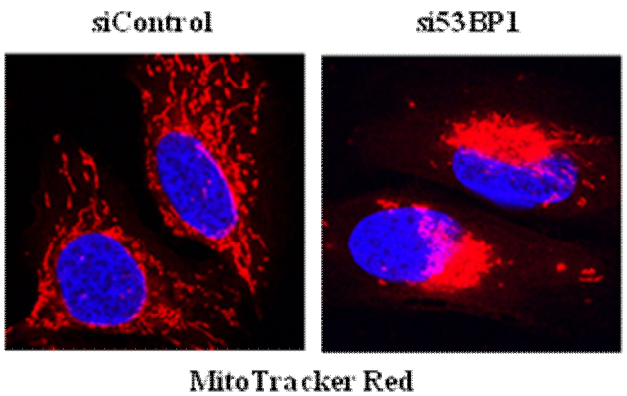
siControl
si53BP1
MitoTracker Red

Figure 4. ROS and Mitochondrial mass levels increased in 53BP1 knockdown cells.

(A) 53BP1-siRNA treated U2OS cells showing increased mitochondrial ROS levels generation was measured by flow cytometry analysis. 53BP1-siRNA: Blue and green two curve, control-siRNA: Red curve, cells labeled with 500 nM MitoTracker® Red CM-H2X ROS for 15 min. The numbers indicate the mean ROS contents for the respective curves (displayed in log scale). (B) 53BP1-siRNA treatment demonstrated increase in mitochondrial mass as assessed by staining with 200 nM MitoTracker® Red CMXRos for 15 min, that binds to mitochondria regardless of their membrane potential. ROS and Mitochondrial mass was determined by quantitative flow cytometry (10,000 enents). (C) mtDNA levels of 53BP1-siRNA U2OS cells were quantified by real-time PCR using primers for mtDNA and nuclear 18S rRNA genes. Mean values are shown ($n \geq 3$ / genotype). (D) The control and 53BP1 knockdown cells were fixed with 4 % paraformaldehydeand and Methanol, stained with 200 nM MitoTracker® Red CMXRos and analyzed by confocal microscopy.

4. 53BP1 deficiency is associated with abnormal mitophagy.

Mitochondria are essential organelles in all eukaryotic cells that direct cellular energy (ATP) production via oxidative phosphorylation. Mitochondria are also major sites of ROS production [40]. Mitochondrial damage were provoked by treatment with the mitochondrial uncoupler CCCP, typically results in autophagic digestion of the damaged mitochondria and leads to reductions in mitochondria and mitochondrial proteins, a process known as mitophagy. The induction of mitophagy after mitochondrial damage is dependent on accumulation of Parkin protein in mitochondria. CCCP treatment of normal human cells led to increased levels of mitochondrial Parkin [41]. Cytochrome *c* oxidase-2 (Cox-2) is a mtDNA-encoded mitochondrial inner membrane protein. Overexpression of Cox-2 leads to phenotypic changes in intestinal epithelial cells that could enhance their tumorigenic potential [48]. We thus investigated function of 53BP1 in the mitochondria. Control-siRNA and 53BP1-siRNA U2OS cells were treated with 20 uM CCCP. Control cells led to slightly increased levels of mitochondria Parkin, and increaced LC3-II levels at the mitochondria, apparently even at higher levels than 53BP1-siRNA cells. 53BP1-siRNA cells did not alter Cox-2, Parkin and LC3-II levels, but Cox-2 and Parkin levels were higher than control-siRNA (Fig. 5). The induction of Cox-2 and Parkin in 53BP1-siRNA cells is dependent abnormal mitophagy. These observations suggest that the process of clearing damaged mitochondria by mitophagy is dependent on 53BP1 proteins. Thus, defective 53BP1 seems to contribute to the increased mitochondrial damage and abnormal mitophagy.

Figure 5.

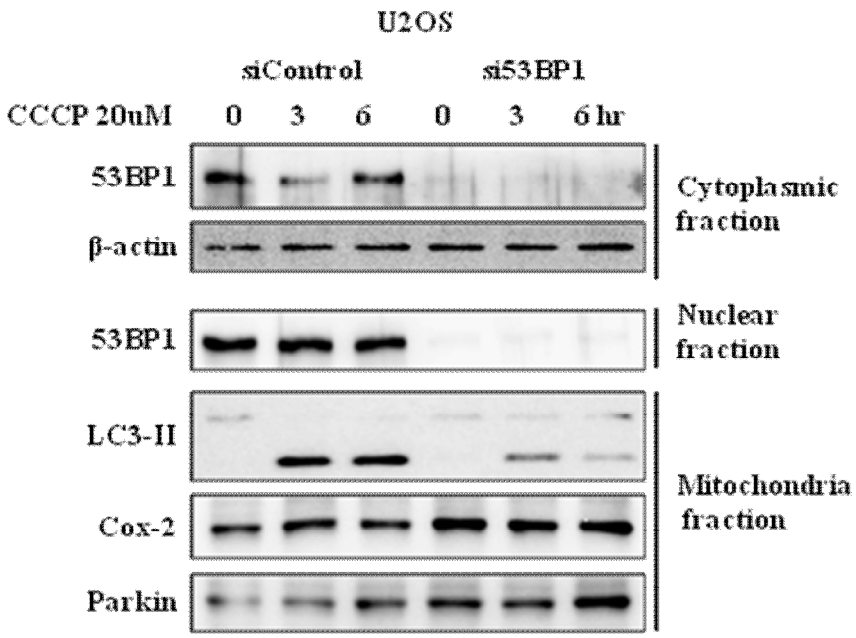

Figure 5. 53BP1 deficiency is associated with abnormal mitophagy.

Mitochondrial protein fractions was analyzed by western blot for the expression of LC3-II (autophagic marker), Parkin and Cox-2. Cells were treated with 20 uM CCCP for 0, 3, 6 hours. Cells were lysed and proteins were isolated followed by immunoblotting against anti-53BP1 and β-actin (loading control) in total cell lysate. β-actin levels in the cytoplasmic fractions of these samples also were analyzed to verify equal loading based on cells.

5. 53BP1 interacts with Foxo3a.

53BP1-Foxo3a association was analyzed by co-immunoprecipitation (co-IP) with the same treatments. We showed that 53BP1 interacts with Foxo3a to form a complex in control cells and that autophagy-related treatments decrease cell death, to identify the signaling pathways responsible for the up-regulation of autophagy-related genes, including LC3 and other, we focused on the role of Foxo3a, since activation of Foxo3a by growth factors is known to inhibit autophagy in different cell types [30]. we investigated regulation of 53BP1 has an essential role in the regulation of the Foxo3a-mediated autophagic signalling pathway after DNA damage induced by H_2O_2. To validate the interaction between 53BP1 and Foxo3a after treatment with H_2O_2 (80uM) for one hour, we compared the levels of Foxo3a and 53BP1 using co-IP and IB assays with cell lysates obtained from HEK 293T cells (Fig. 6A), and U2OS cells were transfected with si53BP1 (Fig. 6B). The results indicate an interaction between 53BP1 and Foxo3a.

Figure 6.

A.

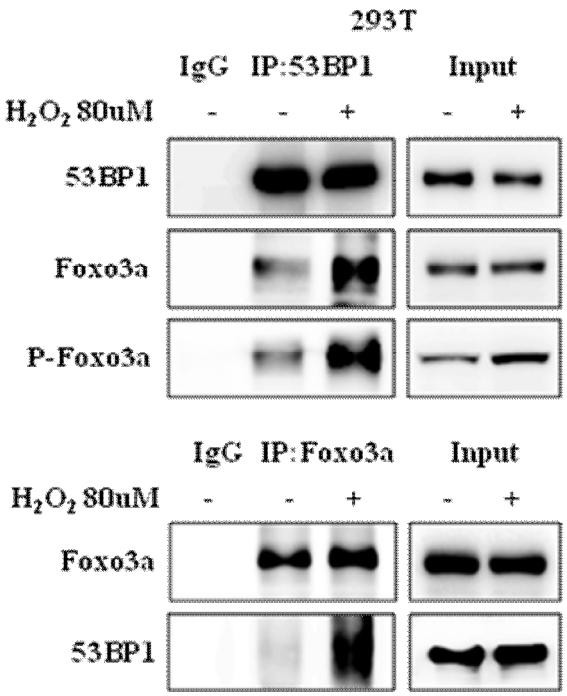
293T
IgG
IP:53BP1
Input
H2O2 80uM
- - + - +
53BP1
Foxo3a
P-Foxo3a
IgG
IP:Foxo3a
Input
H2O2 80uM
- - + - +
Foxo3a
53BP1

B.

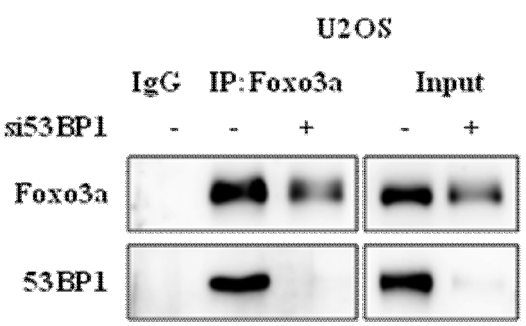
U2OS
IgG
IP:Foxo3a
Input
si53BP1
- - + - +
Foxo3a
53BP1

Figure 6. 53BP1 interacts with Foxo3a proteins.

(A) 53BP1/Foxo3a interaction upon autophagy induction. HEK293T cells were treatment with untreated (-) and H_2O_2 80 uM one hour (+). Protein extracts were subjected to IP with an 53BP1, Foxo3a or as a negative control, with an unrelated antibody (IP IgG). Purified complexes were analyzed together with the corresponding total extracts by western blot (WB) using anti-Foxo3a, p-Foxo3a, 53BP1. (B) U2OS cells trensfected with si53BP1, protein extracts were subjected to IP with an anti-Foxo3a antibody (IP Foxo3a). Purified complexes were analyzed together with the corresponding total extrcts by WB using an anti-Foxo3a, 53BP1.

6. Transcriptional activity of Foxo3a is reduced in 53BP1-silenced cells.

We investigated that 53BP1 affects transcriptional activity of Foxo3a by analysing mRNA levels and using the specific antibody for western blot. Foxo3a protects quiescent cells from oxidative stress by directly increasing their quantities of manganese superoxide dismutase (MnSOD) messenger RNA and protein. This increase in protection from reactive oxygen species antagonizes apoptosis caused by glucose deprivation [36], and Foxo3a increase the expression of antioxidant enzymes catalase [37]. Glutathione peroxidase (GPX) is an antioxidant enzyme that is involved in the control of cellular oxidative state [38]. A transcriptional target of Foxo3a, such as MnSOD, GPX, and LC3 is down-regulated in 53BP1-siRNA cells (Fig. 7A). As well as in Foxo3a-siRNA cells showed decreased MnSOD, GPX, and LC3 mRNA levels (Fig. 7B). Foxo3a has been shown to regulate cell death, and Foxo3a induce Puma transcription [34]. Puma (p53-upregulated modulator of apoptosis) has a role for p53-dependent cell death in the activation. [43]. Puma expression led to a very rapid and profound apoptosis, whereas Puma deficiency promotes resistance to numerous p53-dependent apoptotic stimuli [44, 45]. Activated Foxo3a can inhibit the activation of p53 by DNA damage [46] and Resulted in a significant down-regulation of both p21 and p53 expression in Foxo3a-siRNA U2OS cells but not control cells concurrently, 53BP1-siRNA showed increased p21 and p53 and decreased Puma protein levels than control cells (Fig. 7C). Foxo3a controls the transcription of autophagy-related genes, including LC3 which appears to mediate the effect of Foxo3a on autophagy. The chromatin immunoprecipitation (ChIP) assay is a powerful and versatile technique used for probing protein-DNA interactions within the natural chromatin context of the cell [34]. Therefore, Puma transcriptional factor level in the 53BP1-siRNA cells were lower than control cells (Fig. 8). Taken together, our results suggest that 53BP1 regulates transcriptional activity of Foxo3a transcription factor.

Figure 7.

A.

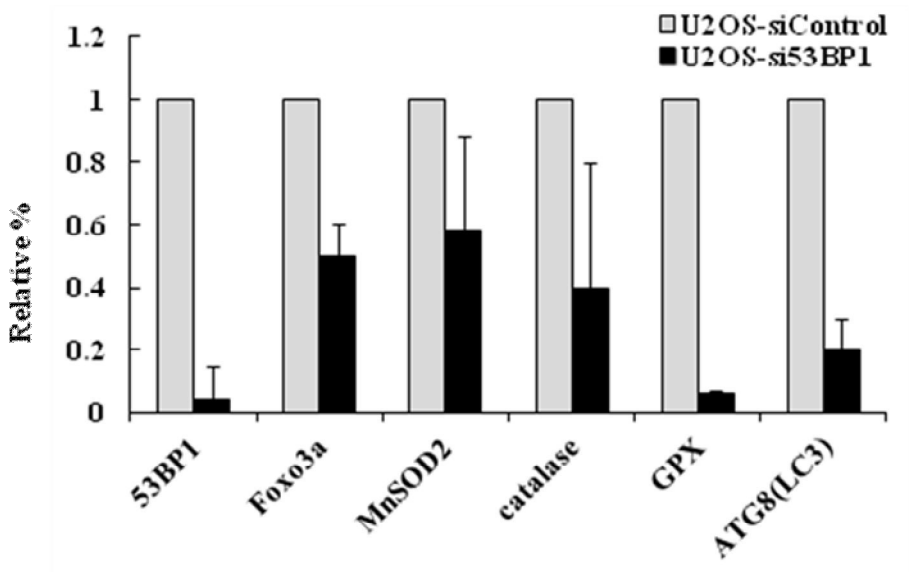
U2OS-siControl
U2OS-si53BP1
Relative %
1.2
1
0.8
0.6
0.4
0.2
0
53BP1
Foxo3a
MnSOD2
catalase
GPX
ATG8(LC3)

B.

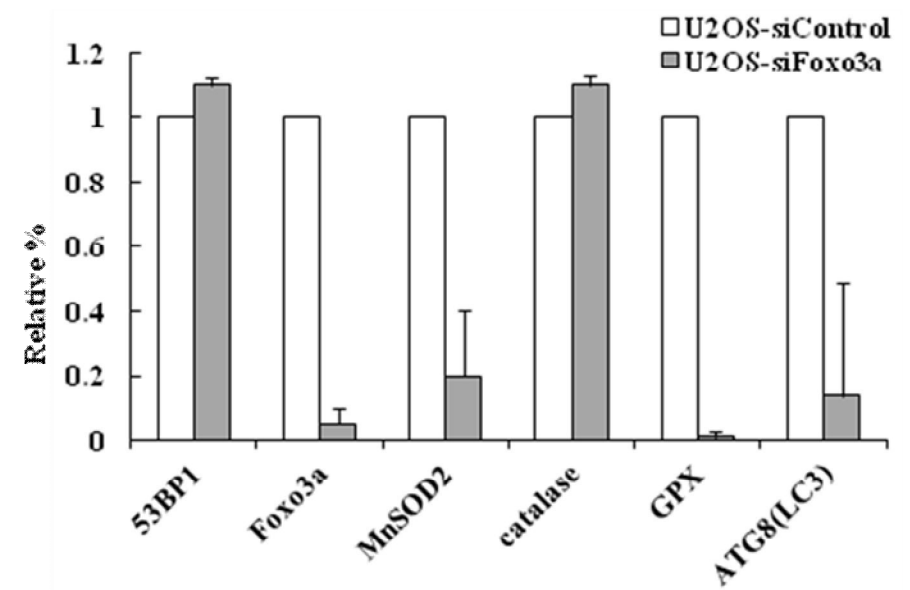
U2OS-siControl
U2OS-siFoxo3a
Relative %
1.2
1
0.8
0.6
0.4
0.2
0
53BP1
Foxo3a
MnSOD2
catalase
GPX
ATG8(LC3)

C.

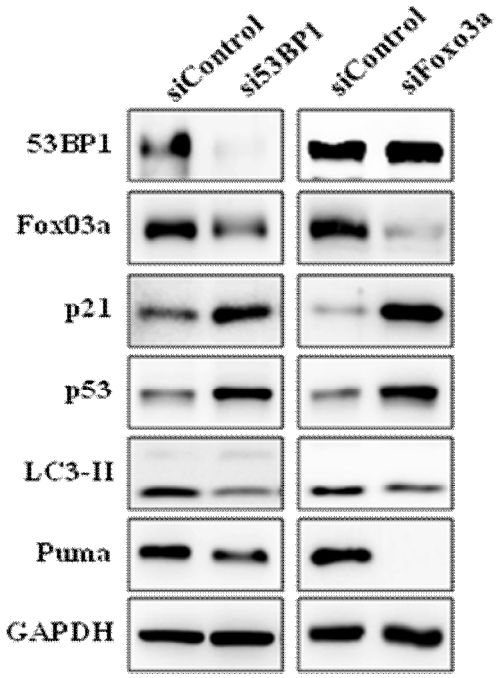

Figure 7. 53BP1 silenced cells inhibited Foxo3a transcriptional factor activity.

Expression of genes involved in Foxo3a transcription function is decreased in U2OS-sicontrol or si53BP1 (A), siFoxo3a (B). 53BP1, Foxo3a, MnSOD, catalase, GPX (glutathione peroxidase) and autophagy pathway genes ATG8 (LC3) mRNA levels is decreased as detected by real-time PCR analyses. mRNA levels were normalized using GAPDH mRNA as an internal control. N.S. indicates not statistically significant. The data was represented as mean ± standard deviation (SD). (C) The proteins were detected by western blot. in 53BP1 and Foxo3a knock down cells compared with controls-siRNA. GAPDH was used as loading control.

Figure 8.

A.

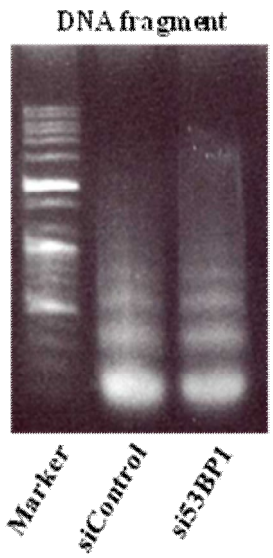

B.

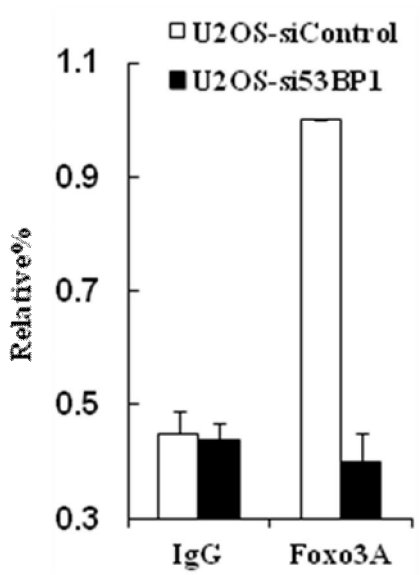

Figure 8. Foxo3a can regulate Puma at the transcriptional levels.

(A) Control-siRNA and 53BP1-siRNA U2OS cells were formaldehyde-crosslinked and chromatin was prepared and digested as described in protocol. Purified DNA 10 μl were separated by electrophoresis on a 1 % agarose gel, and stained with ethidium bromide, shows that the majority of chromatin was digested to 1 to 5 nucleosomes in length (150 to 900 bp). (B) Chromatin immunoprecipitations were performed using digested chromatin from control-siRNA and 53BP1-siRNA U2OS cells and the indicated Foxo3a antibodies. Purified DNA was analyzed by quantitative Real-Time PCR, using Puma FHRE primer. The amount of immunoprecipitated DNA in each sample is represented as signal relative to the total amount of input chromatin.

DISCUSSION

Autophagy is induced by a variety of stress stimuli, including nutrient and energy stress, ER stress, pathogen-associated molecular patterns (PAMPs) and danger-associated molecular patterns (DAMPs), hypoxia, redox stress, and mitochondrial damage. The stimulation of autophagy by these stimuli involves diverse signals that have overlapping functions in autophagy and the control of other cellular stress responses [29]. Autophagy has been shown through activation of LC3-II, a processed form of LC3, is localized in autophagosomes and autolysosomes [25]. 53BP1 was initially identified as a protein that binds to p53 and enhances p53-mediated transcriptional activation [16]. In response to genotoxic stress, 53BP1 rapidly redistributes from a diffuse nuclear localization into distinct nuclear foci suggesting that 53BP1 is involved in the DNA damage response and DNA repair [26].

In this study, we examined the role of 53BP1 in autophagy of U2OS cells. We found that 53BP1-siRNA reduces LC3-I and LC3-II protein levels, and the mitochondrial localization of LC3-II in response to 80 uM H_2O_2 was lower in 53BP1-siRNA transfected cells than in control-siRNA transfectants (Fig. 1). LC3-II is a autophagic marker and Redox regulation of proteins by moderate levels of ROS is observed in autophagy pathway, activation of ROS can elevate autophagy [9, 25]. Our data showed that 53BP1 is key protein in the stimulation of autophagy.

Hydrogen peroxide is known to modulate a variety of cell functions, and its lower biological reactivity compared to many ROS, combined with its capacity to cross membranes and diffuse away from the site of generation, makes it an ideal signalling molecule [55, 56]. ROS can induce apoptosis in many different cell systems. H_2O_2 might be one important trigger mechanism responsible for the short life-span of normal cells [53, 54]. We examined the role of 53BP1 in cytotoxicity of U2OS cells in response to H_2O_2-oxidative stress. The siRNA mediated inhibition of 53BP1 expression decreased the cellular sensitivity to H_2O_2. Survival of

53BP1-siRNA cells following treatment with H_2O_2 and death was determined by the MTT assay. Note the increased viability of the 53BP1-siRNA cells, compared with control-siRNA cells (Fig. 2). Flow cytometry of PI-labeled cells was used to demonstrate a significant increase in the sub-G_1 population in the control-siRNA transfected cells but not in 53BP1-silencing cells (Fig. 3). 53BP1 silencing cells were lower apoptosis to H_2O_2. Apoptosis is associated with the activation of caspases by a cytosolic multiprotein complex formed upon the release of cytochrome *c* from permeabilized mitochondria [57]. This may result in the loss of the mitochondrial membrane potential or the activation of a proapoptotic protein. The release of cytochrome *c* induces the proteolytic activation of procaspase 9 and the downstream activation of caspases-3 and caspase-7 [58]. H_2O_2 induces the cleavage of inactive 32 kDa procaspase-3 into smaller detectable active forms of caspase-3 such as 22 kDa fragments, and the cleavage of inactive 32 kDa procaspase-7 into detectable active forms of caspase-7 such as the 26 kDa fragment, and detectable active forms of caspase-8 and the cleavage of PARP, the proteins were determined by western blot (Fig. 3). Note the increased cleaved forms of caspase proteins in control-siRNA cells, compared with 53BP1-siRNA cells. Therefore, 53BP1 proteins play an important role in autophagy and apoptosis activation. Autophagy appears to act as a death pathway in this analysis because its inhibition results in decreased apoptosis.

The increase in mitochondrial content is associated with defects in the intracellular destruction of abnormal mitochondria (mitophagy) [31]. Importantly, mitochondria are also major sites of ROS production. Oxidative damage can be caused by the ROS produced, that can then damage biologic macromolecules such as lipids, proteins, and DNA [27]. We demonstrate that 53BP1-siRNA cells showed increase in mROS, and mitochondrial mass measured by FACS analysis. Increased mtDNA was measured by RT-PCR and mitochondrial localization was analyzed by confocal microscopy (Fig. 4). These showed that 53BP1 also plays a major role in mitochondrial function and ROS regulation.

Mitochondrial damage provoked by treatment with the mitochondrial uncoupler CCCP typically results in autophagic digestion of the damaged mitochondria and reductions in

mitochondria and mitochondrial proteins, a process known as mitophagy [32]. CCCP treatment of control-siRNA led to increased levels of mitochondrial Parkin (Fig. 5). The induction of mitophagy after mitochondrial damage is dependent on accumulation of Parkin protein in mitochondria. The increased LC3-II after CCCP treatment confirmed that induction of mitochondrial damage increased autophagy in both control-siRNA and 53BP1-siRNA cells, but we showed that the increased LC3-II level was lower in 53BP1-siRNA cells than in control-siRNA cells.

Foxo3a activation results in the repression of a large number of nuclear-encoded genes with mitochondrial function. Superoxide is released into the mitochondrial matrix, where it can be converted into hydrogen peroxide and subsequently into water by SOD2 and catalase (CAT) [35]. In this study, we showed that 53BP1-siRNA U2OS cells revealed increased p21 and p53 protein levels, and decreased MnSOD, GPX, ATG8 (LC3) and Puma mRNA levels by RT-PCR analysis. Also Foxo3a-siRNA cells showed decreased MnSOD, GPX, and LC3 mRNA levels (Fig. 7). Foxo3a up-regulates Puma expression in response to cytokine or growth factor deprivation by ChIP analysis [34]. We found that constitutively active Foxo3a efficiently decrease Puma activity in 53BP1-siRNA U2OS cells (Fig. 8). Thus showing that 53BP1 regulated Foxo3a transcription factor activity.

In conclusion, our study reveals a novel role of 53BP1 in regulating autophagy pathway activity through repression of Foxo3a transcription factor activity. The regulation of 53BP1 gene expression and activity could therefore be important role of autophagy and apoptosis.

REFERENCES

1. N Mizushima, T Yoshimori, B Levine. Methods in mammalian autophagy research. Volume 140, Issue 3, 5 February 2010, Pages 313-326

2. I Tanida, T Ueno, E Kominami LC3 and Autophagy, Volume 445, 2008, pp 77-88.

3. F Reggiori, DJ Klionsky. Autophagy in the Eukaryotic Cell. Eukaryotic Cell February 2002 vol. 1 no. 1 11-21.

4. DJ Klionsky, SD Emr. Autophagy as a Regulated Pathway of Cellular Degradation Science 1 December 2000: Vol. 290 no. 5497 pp. 1717-1721.

5. N Mizushima, T Yoshimori, B Levine. Methods in Mammalian Autophagy Research. Volume 140, Issue 3, 5 February 2010, Pages 313-326.

6. MP Byfield, JT Murray, JM Backer. hVps34 Is a Nutrient-regulated Lipid Kinase Required for Activation of p70 S6 Kinase The Journal of Biological Chemistry, 280, 33076-33082.

7. C Weidinger, K Krause, A Klagge, S Karger and, D Fuhrer. Forkhead box-O transcription factor: critical conductors of cancer's fate. Endocr Relat Cancer December 1, 2008 15 917-929.

8. C Fleury, B Mignotte, JL Vayssière. Mitochondrial reactive oxygen species in cell death signaling. Volume 84, Issues 2-3, February-March 2002, Pages 131-141.

9. R Scherz-Shouval, Z Elazar. ROS, mitochondria and the regulation of autophagy. TRENDS in Cell Biology Vol.17 No.9.

10. H Hongxiang, Z Xiaoning, J Ming. Free radicals and apoptosis.

11. JC Kern, JP Kehrer. Relationships with glutathione, thioredoxin, and the BCL family of proteins Front Biosci, 2005 - bioscience.org

12. J Dorval, A Hontela. Role of glutathione redox cycle and catalase in defense against

oxidative stress induced by endosulfan in adrenocortical cells of rainbow trout (Oncorhynchus mykiss). Volume 192, Issue 2, 15 October 2003, Pages 191-200.

13. G Kopsidas, SA Kovalenko. Tissue Mitochondrial DNA Changes: A Stochastic System. Volume 908, MOLECULAR AND CELLULAR GERONTOLOGY pages 226-243, June 2000.

14. Aubrey D. N. J. de Grey. A proposed refinement of the mitochondrial free radical theory of aging; Myocyte aging and mitochondrial turnover. BioEssays Vol. 19 no. 2 161-167.

15. JAKW Kiel, JA Komduur, IJ van der Klei, M Veenhuis. Macropexophagy in Hansenula polymorpha: facts and views. Volume 549, Issues 1-3, 14 August 2003, Pages 1-6.

16. K Iwabuchi, P L Bartel, B Li, R Marraccino, and S Fields. Two cellular proteins that bind to wild-type but not mutant p53. PNAS June 21, 1994 vol. 91 no. 13 6098-6102.

17. K Iwabuchi, B Li, HF. Massa, BJ. Trask, T Date and S Fields. Stimulation of p53-mediated transcriptional activation by the p53-binding proteins, 53BP1 and 53BP2. 1998 The Journal of Biological Chemistry, 273, 26061-26068.

18. MT Lin, MF Beal. Mitochondrial dysfunction and oxidative stress in neurodegenerative diseases. Nature 443, 787-795 (19 October 2006).

19. RS Balaban, S Nemoto, T Finkel. Mitochondria, Oxidants, and Aging. Volume 120, Issue 4, 25 February 2005, Pages 483-495.

20. M. Flint Beal MD. Mitochondria take center stage in aging and neurodegeneration. Volume 58, Issue 4, pages 495-505, October 2005.

21. GC Kujoth, PC Bradshaw, S Haroon, TA Prolla. The Role of Mitochondrial DNA Mutations in Mammalian Aging. PLoS Genet 3(2): e24. doi:10.1371/journal.pgen.0030024.

22. JR Chapman, MRG Taylor, SJ Boulton. Playing the end game: DNA double-strand break repair pathway choice. Volume 47, Issue 4, 24 August 2012, Pages 497-510.

23. Daniel J. Klionsky and 1269 others. Guidelines for the use and interpretation of assays for monitoring autophagy. Volume 8, Issue 4 April 2012 Pages 445-544.

24. B Levine, G Kroemer. Autophagy in the Pathogenesis of Disease. Volume 132, Issue 1, 11 January 2008, Pages 27-42.

25. Y Kabeya, N Mizushima, T Ueno, A Yamamoto, T Kirisako, T Noda, E Kominami, Y Ohsumi and T Yoshimori. LC3, a mammalian homologue of yeast Apg8p, is localized in autophagosome membranes after processing. The EMBO Journal (2000) 19, 5720-5728.

26. IM Ward, K Minn, KG Jorda, J Chen. Accumulation of Checkpoint Protein 53BP1 at DNA Breaks Involves Its Binding to Phosphorylated Histone H2AX. May 30, 2003 The Journal of Biological Chemistry, 278, 19579-19582.

27. de Moura MB, dos Santos LS, Van HB. Mitochondrial dysfunction in neurodegenerative diseases. and cancer. Environ Mol Mutagen. 2010;51(5):391-405.

28. H Zhang, X Kong, J Kang, J Su, Y Li, J Zhong and L Sun. Oxidative stress induces parallel autophagy and mitochondria dysfunction in human glioma U251 cells. Toxicol. Sci. (2009) 110 (2): 376-388.

29. G Kroemer, G Mariño, B Levine. Autophagy and the Integrated Stress Response. Volume 40, Issue 2, 22 October 2010, Pages 280-293.

30. DAM Salih, A Brunet. FoxO transcription factors in the maintenance of cellular homeostasis during aging. Volume 20, Issue 2, April 2008, Pages 126-136.

31. YA. Valentin-Vega, KH. MacLean, JTait-Mulder, S Milasta, M Steeves, FC. Dorsey, John L. Cleveland, DR. Green and MB. Kastan. Mitochondrial dysfunction in ataxia-telangiectasia Blood February 9, 2012 vol. 119 no. 6 1490-1500.

32. RJ Youle, DP Narendra. Mechanisms of mitophagy. Nature Reviews Molecular Cell Biology 12, 9-14 (January 2011).

33. T Yahata, T Takanashi, Y Muguruma, Abd Aziz Ibrahim, H Matsuzawa, T Uno, Y Sheng,

M Onizuka, M Ito, S Kato and K Ando. Accumulation of oxidative DNA damage restricts the self-renewal capacity of human hematopoietic stem cells. Blood September 15, 2011 vol. 118 no. 11 2941-2950.

34. H You, M Pellegrini, K Tsuchihara, K Yamamoto, G Hacker, M Erlacher, A Villunger and T W. Mak. FOXO3a-dependent regulation of Puma in response to cytokine-growth factor withdrawal. Published June 26, 2006 // JEM vol. 203 no. 7 1657-1663.

35. E C Ferber, B Peck, O Delpuech, G P Bell, P East and A Schulze. FOXO3a regulates reactive oxygen metabolism by inhibiting mitochondrial gene expression. Cell Death and Differentiation (2012) 19, 968-979.

36. Geert J. P. L. Kops, Tobias B. Dansen, Paulien E. Polderman, Ingrid Saarloos, Karel W. A. Wirtz, Paul J. Coffer, Ting-T. Huang, Johannes L. Bos, René H. Medema & Boudewijn M. T. Burgering. Forkhead transcription factor FOXO3a protects quiescent cells from oxidative stress. Nature 419, 316-321 (19 September 2002).

37. CB. Chiribau, L Cheng, IC. Cucoranu, Y-S Yu, R E. Clempus and Dan Sorescu FOXO3A Regulates Peroxiredoxin III Expression in Human Cardiac Fibroblasts. March 28, 2008 The Journal of Biological Chemistry, 283, 8211-8217.

38. PJ. Crack, JM. Taylor, NJ. Flentjar, Judy de Haan,P Hertzog, RC. Iannello and I Kola. Increased infarct size and exacerbated apoptosis in the glutathione peroxidase1 (Gpx-1) knockout mouse brain in response to ischemia/reperfusion injury. Journal of Neurochemistry, 2001, 78, 1389-1399

39. Y Kurihara, T Kanki1, Y Aoki, Y Hirota, T Saigusa, T Uchiumi, and D Kang. Mitophagy Plays an Essential Role in Reducing Mitochondrial Production of Reactive Oxygen Species and Mutation of Mitochondrial DNA by Maintaining Mitochondrial Quantity and Quality in Yeast. THE JOURNAL OF BIOLOGICAL CHEMISTRY VOL. 287, NO. 5, pp. 3265-3272, January 27, 2012.

40. Van Houten B, Woshner V, Santos JH. Role of mitochondrial DNA in toxic responses to oxidative stress. DNA Repair. 2006;5(2):145-152.

41. Youle RJ, Narendra DP. Mechanisms of mitophagy. Nat Rev Mol Cell Biol. 2011;12(1):9-14.

42. N. Mizushima et al., J. Dissection of Autophagosome Formation Using Apg5-Deficient Mouse Embryonic Stem Cells. Cell Biol. 152, 657 (2001).

43. K Nakano, KH Vousden. PUMA, a Novel Proapoptotic Gene, Is Induced by p53. Molecular Cell, Vol. 7, 683-694, March, 2001.

44. J Yu, L Zhang, PM Hwang, KW Kinzler, B Vogelstein. PUMA induces the rapid apoptosis of colorectal cancer cells. Molecular Cell, Vol. 7, 673-682, March, 2001.

45. JE Chipuk, L Bouchier-Hayes, T Kuwana. PUMA couples the nuclear and cytoplasmic proapoptotic function of p53. SCIENCE VOL 309 9 SEPTEMBER 2005

46. H You, K Yamamoto, TW Mak. Regulation of transactivation-independent proapoptotic activity of p53 by FOXO3a. PNAS June 13, 2006 vol. 103 no. 24 9051-9056.

47. Gomez-Santos, C. et al. (2003) Dopamine induces autophagic cell death and alpha-synuclein increase in human neuroblastoma SH-SY5Y cells. J. Neurosci. Res. 73, 341-350.

48. M. Tsujii, R.N. DuBois, Alterations in cellular adhesion and apoptosis in epithelial cells overexpressing prostaglandin endoperoxide synthase 2, Cell 83 (1995) 493-501.

49. A Alexander, SL Cai, J Kim, A Nanez…ATM signals to TSC2 in the cytoplasm to regulate mTORC1 in response to ROS. PNAS March 2, 2010 vol. 107 no. 9 4153-4158.

50. R Kang, H J Zeh, M T Lotze and D Tang. The Beclin 1 network regulates autophagy and apoptosis. Cell Death and Differentiation (2011) 18, 571-580.

51. N Hay, N Sonenberg. Upstream and downstream of mTOR. GENES & DEVELOPMENT 18:1926-1945.

52. Shintani T, Klionsky DJ (2004) Autophagy in health and disease: A double-edged sword. Science 306:990-995.

53. Watson RW, Rotstein OD, Jimenez M, Parodo J, Marshall JC. Augmented intracellular glutathione inhibits Fas-triggered apoptosis of activated human neutrophils. Blood 1997; 89: 4175-4181.

54. H.-U. Simon, A. Haj-Yehia and F. Levi-Schaffer. Role of reactive oxygen species (ROS) in apoptosis induction. Apoptosis 2000; 5: 415-418.

55. MB Hampton, S Orrenius. Dual regulation of caspase activity by hydrogen peroxide: implications for apoptosis. FEBS Letters 414 (1997) 552-556.

56. Suzuki, Y.J., Forman, H.J. and Sevanian, A. (1997) Free Radical Biol. Med. 22, 269-285.

57. Garrido C, Galluzzi L, Brunet M, Puig PE, Didelot C, Kroemer G. Mechanisms of cytochrome c release from mitochondria. Cell Death Differ 2006;13(9):1423-33.

58. Norbury CJ, Zhivotovsky B. DNA damage-induced apoptosis. Oncogene 2004;23(16):2797-808.

59. C Dudgeon, P Wang, X Sun, et al. PUMA Induction by FoxO3a Mediates the Anticancer Activities of the Broad-Range Kinase Inhibitor UCN-01. Mol Cancer Ther 2010;9:2893-2902.

<국문초록>

53BP1에 의한 autophagy 유발기작 규명연구

공 옥 화

지도교수 : 유 호 진

조선대학교 대학원 생물신소재학과

Foxo3a 는 Forkhead box-O 전사 인자 그룹의 구성원이고, DNA 손상 복구, 세포 사멸, autophagy 와 기타 다른 세포내의 유전자의 발현 조절 과정에 관련된다. Foxo3a 의 아세틸레이션은 세포 내의 산화 스트레스 반응에서 증가된다. 아세틸의 정확한 결과는 불분명하지만 최근 CBP 및 / 또는 P300 에 의한 Foxo3a 인자의 아세틸레이션은 새로운 규제 경로로 확인되었다. 본 연구에서, 우리는 Foxo3a 단백질이 53BP1 과 결합하여 autophagy 를 조절하는 것을 보여준다. Foxo3a 는 autophagy 와 세포 사멸 관련 유전자의 전사를 조절한다. 우리는 포유 동물 세포에서 siRNA 를 사용하여 53BP1 를 억제하므로 Foxo3a 의 전사 조절 유전자들이 억제됨을 확인하였다. 게다가 53BP1-siRNA U2OS 세포에서 Foxo3a 의 활성을 증가시키므로 Puma 활성이 감소 되는 것으로 나타났다. 53BP1 이 억제된 세포는 autophagy 를 감소시키고, ROS 와 미토콘드리아 질량을 증가시켰다. H_2O_2 를 처리하였을 때, 53BP1 을 억제한 세포에서는 viability 가 증가하였다. 또한, 53BP1 억제는 Foxo3a 전사 인자의 활성화를 추진 하였다. 결론적으로, 우리의 연구는 53BP1 이 Foxo3a 전사 인자 기능을 조절하므로서 autophagy 를 조절하는 새로운 역할이 있음을 보여준다.

저작물 이용 허락서

학 과	생물신소재학과	학 번	20117758	과 정	석 사
성 명	한글 : 공 옥 화 한문 : 孔 玉 花 영문 : Yu Hua Kong				
주 소	광주광역시 동구 서석동 조선대학교 그린빌리지				
연락처	E-MAIL : jamie2701@gmail.com				
논문제목	한글: 53BP1에 의한 autophagy 유발기작 규명연구 영문: The dynamic interaction of Foxo3a with the 53BP1 regulates mammalian autophagy				

본인이 저작한 위의 저작물에 대하여 다음과 같은 조건아래 조선대학교가 저작물을 이용할 수 있도록 허락하고 동의합니다.

- 다 음 -

1. 저작물의 DB구축 및 인터넷을 포함한 정보통신망에의 공개를 위한 저작물의 복제, 기억장치에의 저장, 전송 등을 허락함
2. 위의 목적을 위하여 필요한 범위 내에서의 편집·형식상의 변경을 허락함. 다만, 저작물의 내용변경은 금지함.
3. 배포·전송된 저작물의 영리적 목적을 위한 복제, 저장, 전송 등은 금지함.
4. 저작물에 대한 이용기간은 5년으로 하고, 기간종료 3개월 이내에 별도의 의사표시가 없을 경우에는 저작물의 이용기간을 계속 연장함.
5. 해당 저작물의 저작권을 타인에게 양도하거나 또는 출판을 허락을 하였을 경우에는 1개월 이내에 대학에 이를 통보함.
6. 조선대학교는 저작물의 이용허락 이후 해당 저작물로 인하여 발생하는 타인에 의한 권리 침해에 대하여 일체의 법적 책임을 지지 않음
7. 소속대학의 협정기관에 저작물의 제공 및 인터넷 등 정보통신망을 이용한 저작물의 전송·출력을 허락함.

동의여부 : 동의(0) 반대( )

2013년 5 월 일

저작자: 공 옥 화 (서명 또는 인)

조선대학교 총장 귀하